



Aaij, R. et al. (2012) Observation of excited Λ_b^0 baryons. Physical Review Letters, 109 (17). Art. 172003. ISSN 0031-9007

Copyright © 2012 CERN, for the benefit of the LHCb collaboration

<http://eprints.gla.ac.uk/80213/>

Deposited on: 13 June 2013

Enlighten – Research publications by members of the University of Glasgow
<http://eprints.gla.ac.uk>



Observation of Excited Λ_b^0 Baryons

R. Aaij *et al.**

(LHCb Collaboration)

(Received 16 May 2012; published 26 October 2012)

Using pp collision data corresponding to 1.0 fb^{-1} integrated luminosity collected by the LHCb detector, two narrow states are observed in the $\Lambda_b^0 \pi^+ \pi^-$ spectrum with masses $5911.97 \pm 0.12(\text{stat}) \pm 0.02(\text{syst}) \pm 0.66(\Lambda_b^0 \text{ mass}) \text{ MeV}/c^2$ and $5919.77 \pm 0.08(\text{stat}) \pm 0.02(\text{syst}) \pm 0.66(\Lambda_b^0 \text{ mass}) \text{ MeV}/c^2$. The significances of the observations are 5.2 and 10.2 standard deviations, respectively. These states are interpreted as the orbitally excited Λ_b^0 baryons, $\Lambda_b^{*0}(5912)$ and $\Lambda_b^{*0}(5920)$.

DOI: [10.1103/PhysRevLett.109.172003](https://doi.org/10.1103/PhysRevLett.109.172003)

PACS numbers: 14.20.Mr, 13.30.Eg, 13.60.Rj

The system of baryons containing a b quark (beauty baryons) remains largely unexplored, despite recent progress made at the experiments at the Tevatron. In addition to the ground state Λ_b^0 , the Ξ_b^- baryon with the quark content bsd has been observed by the D0 [1] and CDF [2] Collaborations, followed by the observation of the doubly strange Ω_b^- baryon (bss) [3,4]. The last ground state of beauty-strange content, Ξ_b^0 (bsu), has been observed by CDF [5]. Recently, the CMS Collaboration has found the corresponding excited state, most likely Ξ_b^{*0} with $J^P = 3/2^+$ [6]. Beauty baryons with two light quarks (bqq , where $q = u, d$), other than the Λ_b^0 , have been studied so far by CDF only. Of the triplets $\Sigma_b^{\pm,0}$ with spin $J = 1/2$ and $\Sigma_b^{*\pm,0}$ with $J = 3/2$ predicted by theory, only the charged states $\Sigma_b^{(*)\pm}$ have so far been observed via their decay to $\Lambda_b^0 \pi^\pm$ final states [7,8]. None of the quantum numbers of beauty baryons have been measured.

The quark model predicts the existence of two orbitally excited Λ_b^0 states Λ_b^{*0} , with the quantum numbers $J^P = 1/2^-$ and $3/2^-$, respectively, that should decay to $\Lambda_b^0 \pi^+ \pi^-$ or $\Lambda_b^0 \gamma$. These states have not previously been established experimentally. The properties of excited Λ_b^0 baryons are discussed in Refs. [9–15]. Most predictions give masses above the $\Lambda_b^0 \pi^+ \pi^-$ threshold but below the $\Sigma_b \pi$ threshold. Observation of Λ_b^{*0} states and measurement of their quantum numbers would provide a further confirmation of the validity of the quark model, and the precise measurement of their masses would test the applicability of various theoretical models used to describe the interaction of heavy quarks.

This Letter reports the first observation of the Λ_b^{*0} states decaying into $\Lambda_b^0 \pi^+ \pi^-$ and the measurement of their masses and upper limits on their natural widths. The data

set of 1.0 fb^{-1} collected in pp collisions at the LHC at the center-of-mass energy $\sqrt{s} = 7 \text{ TeV}$ in 2011 is used for the analysis.

The LHCb detector [16] is a single-arm forward spectrometer covering the pseudorapidity range $2 < \eta < 5$, designed for the study of particles containing b or c quarks. The detector includes a high precision tracking system consisting of a silicon-strip vertex detector surrounding the pp interaction region, a large-area silicon-strip detector located upstream of a dipole magnet with a bending power of about 4 Tm, and three stations of silicon-strip detectors and straw drift tubes placed downstream. The combined tracking system has a momentum resolution $\Delta p/p$ that varies from 0.4% at 5 GeV/ c to 0.6% at 100 GeV/ c and an impact parameter (IP) resolution of 20 μm for tracks with high transverse momentum. Charged hadrons are identified by using two ring-imaging Cherenkov detectors. Photon, electron, and hadron candidates are identified by a calorimeter system consisting of scintillating-pad and pre-shower detectors, an electromagnetic calorimeter, and a hadronic calorimeter. Muons are identified by a muon system composed of alternating layers of iron and multi-wire proportional chambers.

The online event selection (trigger) consists of a hardware stage, based on information from the calorimeter and muon systems, followed by a software stage which applies full event reconstruction. The software trigger used in this analysis requires a two-, three-, or four-track secondary vertex with a high sum of the momenta transverse to the beam axis, p_T , of the tracks, and significant displacement from the primary interaction vertex (PV). In addition, the secondary vertex should have at least one track with $p_T > 1.7 \text{ GeV}/c$, IP χ^2 with respect to any PV greater than 16 (where the IP χ^2 is defined as the difference of the PV fit χ^2 with and without the track included), and a track fit $\chi^2/\text{ndf} < 2$, where ndf is the number of degrees of freedom in the fit. A multivariate algorithm is used for the identification of the secondary vertices [17].

The Λ_b^{*0} candidates are reconstructed in the $\Lambda_b^0 \rightarrow \Lambda_c^+ \pi^-$, $\Lambda_c^+ \rightarrow p K^- \pi^+$ decay chain (addition of charge-conjugate states is implied throughout this Letter). The

*Full author list given at the end of the article.

Published by the American Physical Society under the terms of the [Creative Commons Attribution 3.0 License](https://creativecommons.org/licenses/by/3.0/). Further distribution of this work must maintain attribution to the author(s) and the published article's title, journal citation, and DOI.

selection of Λ_b^0 candidates is performed in two stages. First, a loose preselection of events containing beauty hadron candidates decaying to charm hadron candidates is performed. It requires that the tracks forming the candidate, as well as the beauty and charm vertices, have good quality and are well separated from any PV, and the invariant masses of the beauty and charm candidates are consistent with the masses of the corresponding particles.

The final selection requires that all the tracks forming the Λ_b^0 candidate have an IP χ^2 with respect to any PV greater than 9, and the IP χ^2 of the Λ_b^0 candidate to the best PV (PV having the minimum IP χ^2 for the Λ_b^0 candidate) is less than 16. Particle identification (PID) information from the ring-imaging Cherenkov detectors is used to identify kaons and protons in the final state in the form of differences of logarithms of likelihoods between the proton and pion ($DLL_{p\pi}$) and kaon and pion ($DLL_{K\pi}$) hypotheses. No PID requirements are applied to the pions from $\Lambda_b^0 \rightarrow \Lambda_c^+ \pi^-$ decays to increase the Λ_b^0 yield: A significant fraction of these pions have momenta above 100 GeV/c, where the PID performance is reduced. Finally, a kinematic fit is used which constrains the decay products of the Λ_b^0 and Λ_c^+ baryons to originate from common vertices, the Λ_b^0 to originate from the PV, and the invariant mass of the Λ_c^+ candidate to be equal to the established Λ_c^+ mass [18].

A momentum scale correction is applied to all invariant mass spectra in this analysis to improve the mass measurement using the procedure similar to Ref. [19]. The momentum scale has been calibrated by using $J/\psi \rightarrow \mu^+ \mu^-$ decays, and its accuracy has been quantified with other two-body resonance decays [$Y(1S) \rightarrow \mu^+ \mu^-$, $K_S^0 \rightarrow \pi^+ \pi^-$, $\phi \rightarrow K^+ K^-$].

Signal and background distributions are studied by using simulation. Proton-proton collisions are generated by using PYTHIA 6.4 [20] with a specific LHCb configuration [21]. Decays of hadronic particles are described by EVTGEN [22] in which final state radiation is generated by using PHOTOS [23]. The interaction of the generated particles with the detector and its response are implemented by using the GEANT4 toolkit [24] as described in Ref. [25].

The distribution of the $\Lambda_c^+ \pi^-$ invariant mass after the kinematic fit is shown in Fig. 1, where a requirement of good quality of the kinematic fit is applied. In addition to the $\Lambda_b^0 \rightarrow \Lambda_c^+ \pi^-$ signal contribution, the spectrum contains backgrounds from random combinations of tracks (random background), from partially reconstructed decays where one or more particles are not reconstructed, and from $\Lambda_b^0 \rightarrow \Lambda_c^+ K^-$ decays with the kaon reconstructed under the pion mass hypothesis. A fit of the spectrum yields 70540 ± 330 signal events, and the signal-to-background ratio in a ± 25 MeV/ c^2 interval around the nominal Λ_b^0 mass is $S/B = 11$. The fit to the $\Lambda_c^+ \pi^-$ spectrum is used only to estimate the Λ_b^0 yield and the $\Lambda_b^0 \rightarrow \Lambda_c^+ K^-$ contribution and is not used in the subsequent analysis.

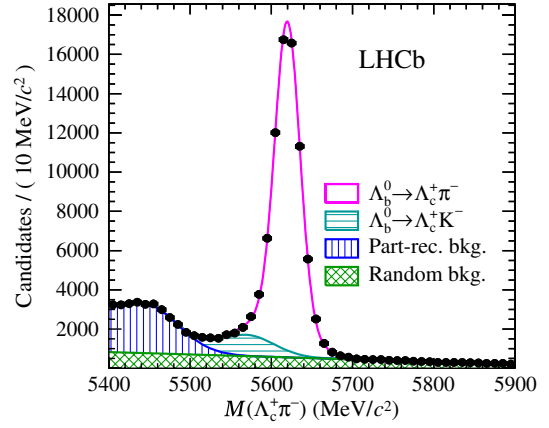


FIG. 1 (color online). Invariant mass spectrum of $\Lambda_c^+ \pi^-$ combinations. The points with error bars are the data, and the fitted $\Lambda_b^0 \rightarrow \Lambda_c^+ \pi^-$ signal and three background components ($\Lambda_b^0 \rightarrow \Lambda_c^+ K^-$, partially reconstructed, and random background) are shown with different fill styles.

The Λ_b^0 candidates obtained with the above selection are combined with two tracks under the pion mass hypothesis (referred to as slow pions from now on) to search for excited Λ_b^0 states. The tracks are required to have transverse momentum $p_T > 150$ MeV/c, and no PID requirements are applied. A kinematic fit is applied that, in addition to all constraints described above for Λ_b^0 candidates, constrains the two slow pion tracks to originate from the PV and the invariant mass of the Λ_b^0 candidate to a fixed value of 5619.37 MeV/ c^2 , which is a combination of the world average [18] and the LHCb measurement [26]. The uncertainty on the combined Λ_b^0 mass obtained in this way, 0.69 MeV/ c^2 , is treated as a systematic effect. Combinations with a good quality of kinematic fit, $\chi^2/\text{ndf} < 3.3$, are retained. From the simulation study, this requirement is optimal for the observation of a narrow state near the kinematic threshold with a signal-to-background ratio around one.

The fit of the $\Lambda_c^+ \pi^-$ mass spectrum (Fig. 1) indicates the presence of the background from $\Lambda_b^0 \rightarrow \Lambda_c^+ K^-$ decays at a rate around 12%, relative to the $\Lambda_b^0 \rightarrow \Lambda_c^+ \pi^-$ signal. Alternatively, its rate can be estimated from the ratio of $B^+ \rightarrow \bar{D}^0 K^+$ and $B^+ \rightarrow \bar{D}^0 \pi^+$ decays that equals 8% [18]. Because of the Λ_b^0 mass constraint in the kinematic fit, the $\Lambda_b^0 \pi^+ \pi^-$ invariant mass distribution for this mode is biased by less than 0.1 MeV/ c^2 if reconstructed under the $\Lambda_c^+ \pi^-$ mass hypothesis and has a resolution only a factor of 2 worse than that with the $\Lambda_c^+ \pi^-$ signal. After the kinematic fit quality requirement, the fraction of $\Lambda_b^0 \pi^+ \pi^-$ with $\Lambda_b^0 \rightarrow \Lambda_c^+ K^-$ decays compared to those with the $\Lambda_c^+ \pi^-$ is reduced to 8%. This mode is thus not treated separately, and its effect is taken into account as a part of the systematic uncertainty due to the signal shape.

Combinations of Λ_b^0 candidates with both opposite-sign and same-sign slow pions are selected in the data. The

latter are used to constrain the background shape coming from random combinations of the Λ_b^0 baryon and two tracks. The assumption that the shape of the background in $\Lambda_b^0 \pi^+ \pi^-$ and $\Lambda_b^0 \pi^\pm \pi^\pm$ modes is the same is validated with simulation. The $\Lambda_b^0 \pi^+ \pi^-$ and $\Lambda_b^0 \pi^\pm \pi^\pm$ invariant mass spectra are shown in Fig. 2; two narrow structures with masses around 5912 and 5920 MeV/ c^2 are evident in the $\Lambda_b^0 \pi^+ \pi^-$ spectrum. They are interpreted as the orbitally excited Λ_b^0 states and are denoted hereafter as $\Lambda_b^{*0}(5912)$ and $\Lambda_b^{*0}(5920)$.

A combined unbinned fit of the $\Lambda_b^0 \pi^+ \pi^-$ and $\Lambda_b^0 \pi^\pm \pi^\pm$ samples is performed to extract the masses and event yields of the two states. The background is described with a quadratic polynomial function with common parameters for both samples except for an overall normalization. The probability density function (PDF) for each of the $\Lambda_b^{*0}(5912)$ and $\Lambda_b^{*0}(5920)$ signals is a sum of two Gaussian PDFs with the same mean. The relative normalizations of the two Gaussian PDFs are fixed to the values obtained from the simulation of states with masses 5912 and 5920 MeV/ c^2 and zero natural widths, while the mean value and overall normalization for each signal are left free in the fit. The core resolution (width of the narrower Gaussian PDF) obtained from simulation is 0.19 and 0.27 MeV/ c^2 for $\Lambda_b^{*0}(5912)$ and $\Lambda_b^{*0}(5920)$, respectively. Study of several high-statistics samples [$\Lambda_b^0 \rightarrow \Lambda_c^+ \pi^-$, $\psi(2S) \rightarrow J/\psi \pi^+ \pi^-$, $D^{*+} \rightarrow D^0 \pi^+$] shows that the invariant mass resolution in the data is typically worse by 20% than in the simulation. Thus the nominal data fit uses

the widths of Gaussian PDFs from the simulation multiplied by 1.2. The data fit yields 17.6 ± 4.8 events with mass $M_{\Lambda_b^{*0}(5912)} = 5911.97 \pm 0.12$ MeV/ c^2 and 52.5 ± 8.1 events with mass $M_{\Lambda_b^{*0}(5920)} = 5919.77 \pm 0.08$ MeV/ c^2 .

Limits on natural widths Γ of the two states are obtained by performing an alternative fit where the signal PDFs are convolved with relativistic Breit-Wigner distributions. The dependence of Breit-Wigner width Γ on the $\Lambda_b^0 \pi^+ \pi^-$ invariant mass M is taken into account as $\Gamma_{\Lambda_b^{*0}}(M) = \Gamma_{\Lambda_b^{*0}} \times (q/q_0)^2 \times (M_{\Lambda_b^{*0}}/M)$. Here $M_{\Lambda_b^{*0}}$ is the mass of the Λ_b^{*0} state, and $q_{(0)}$ is the kinematic energy for the decay of the state with mass $M_{(\Lambda_b^{*0})}$: $q_{(0)} = M_{(\Lambda_b^{*0})} - M_{\Lambda_b^0} - 2M_\pi$, where $M_{\Lambda_b^0}$ and M_π are the masses of Λ_b^0 and π^+ , respectively. Scans of Breit-Wigner widths $\Gamma_{\Lambda_b^{*0}(5912)}$ and $\Gamma_{\Lambda_b^{*0}(5920)}$ are performed with all the other parameters free to vary in the fit. The upper limits are obtained without applying the mass resolution scaling factor of 1.2 as in the nominal fit to account for the uncertainty of this quantity: This gives a more conservative value for the upper limit. The 90% (95%) confidence level (C.L.) upper limit on Γ , which corresponds to 1.28 (1.64) standard deviations, is obtained as the value of Γ where the negative logarithm of the likelihood is $1.28^2/2 = 0.82$ ($1.64^2/2 = 1.34$) greater than at its minimum. The 90% (95%) C.L. upper limit is $\Gamma_{\Lambda_b^{*0}(5912)} < 0.66$ MeV (0.83 MeV) for the $\Lambda_b^{*0}(5912)$ state and $\Gamma_{\Lambda_b^{*0}(5920)} < 0.63$ MeV (0.75 MeV) for the $\Lambda_b^{*0}(5920)$ state.

The invariant mass of the two pions, $M(\pi^+ \pi^-)$, in the $\Lambda_b^{*0}(5920) \rightarrow \Lambda_b^0 \pi^+ \pi^-$ decay is shown in Fig. 3. The background is subtracted by using the SWEIGHTS procedure [27]. The weights are calculated from the fit to $\Lambda_b^0 \pi^+ \pi^-$ invariant mass distribution, which is practically uncorrelated with $M(\pi^+ \pi^-)$. The $M(\pi^+ \pi^-)$ distribution is consistent with the result of phase-space decay simulation, with $\chi^2/\text{ndf} = 1.6$ for $\text{ndf} = 9$. No peaking structures are evident.

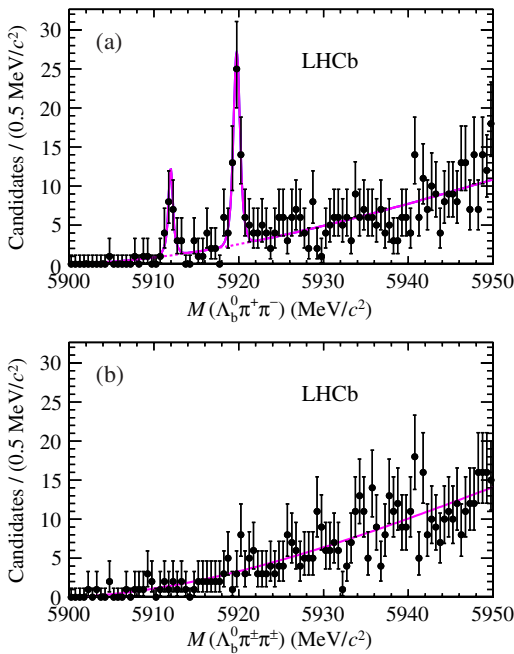


FIG. 2 (color online). Invariant mass spectrum of (a) $\Lambda_b^0 \pi^+ \pi^-$ and (b) $\Lambda_b^0 \pi^\pm \pi^\pm$ combinations. The points with error bars are the data, the solid line is the fit result, and the dashed line is the background contribution.

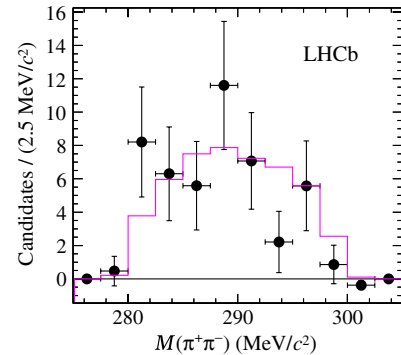


FIG. 3 (color online). Invariant mass of the two pions from $\Lambda_b^{*0}(5920) \rightarrow \Lambda_b^0 \pi^+ \pi^-$ decay. The points with the error bars are background-subtracted data, and the solid histogram is the result of phase-space decay simulation.

TABLE I. Systematic uncertainties on the mass difference $\Delta M_{\Lambda_b^{*0}}$ between Λ_b^{*0} and Λ_b^0 .

Source of uncertainty	Systematic bias (MeV/ c^2)	
	$\Delta M_{\Lambda_b^{*0}(5912)}$	$\Delta M_{\Lambda_b^{*0}(5920)}$
Λ_b^0 mass	0.034	0.035
Signal PDF	0.021	0.011
Background PDF	0.002	0.002
Momentum scale	0.008	0.013
Total	0.041	0.039

Systematic uncertainties on the mass measurement are shown in Table I. The dominant uncertainty in the absolute Λ_b^{*0} mass measurement comes from the uncertainty on the Λ_b^0 mass $\delta M_{\Lambda_b^0} = 0.69$ MeV/ c^2 ; it is propagated to the Λ_b^{*0} mass uncertainty as $\delta M_{\Lambda_b^{*0}} = \delta M_{\Lambda_b^0} \times (M_{\Lambda_b^0}/M_{\Lambda_b^{*0}}) \approx 0.66$ MeV/ c^2 . This uncertainty mostly cancels in the mass difference $\Delta M_{\Lambda_b^{*0}} = M_{\Lambda_b^{*0}} - M_{\Lambda_b^0}$, where the residual uncertainty is $\delta \Delta M_{\Lambda_b^{*0}} = \delta M_{\Lambda_b^0} \times (\Delta M_{\Lambda_b^0}/M_{\Lambda_b^{*0}})$. The uncertainty of the signal parameterization is estimated by using the simulated signal parametrization without applying the resolution scaling factor, by using the natural width for both states when left free in the fit, and by conservatively including the $\Lambda_b^0 \rightarrow \Lambda_c^+ K^-$ contribution with the rate 12% parameterized from simulation. The uncertainty due to the background parameterization is estimated by (i) using an alternative fit model for background description, (ii) using the fit without the $\Lambda_b^0 \pi^\pm \pi^\pm$ constraint, (iii) using the fit with the background obtained from the simulation, (iv) fitting in the reduced invariant mass range 5910–5930 MeV/ c^2 , and (v) taking the largest difference from the nominal fit result as a systematic uncertainty. The effect of the momentum scale correction is evaluated by varying the scale coefficient by its relative uncertainty 5×10^{-4} in simulated signal samples.

The significance of the observation of the two states is evaluated with simulated pseudoexperiments. A large number of background-only invariant mass distributions are simulated with parameters equal to the fit result, and each distribution is fitted with models that include background only, as well as background and signal. The mean mass value of the signal PDF is not constrained in the fit to account for a trial factor in the range 5900–5950 MeV/ c^2 . The significance is calculated as the fraction of samples where the difference of the logarithms of fit likelihoods $\Delta \log \mathcal{L}$ with and without the signal is larger than in the data. The fraction is obtained by an exponential extrapolation of the $\Delta \log \mathcal{L}$ distribution [28] that allows a limited number of pseudoexperiments to be used for a signal with high significance. The significance is then expressed in terms of the number of standard deviations (σ). The significance of the $\Lambda_b^{*0}(5912)$ state obtained in this way is 5.4σ for the $\Delta \log \mathcal{L}$ obtained from the nominal fit. To account for systematic effects, the minimum $\Delta \log \mathcal{L}$

among all systematic variations is taken; in that case, the significance reduces to 5.2σ . Similarly, the statistical significance of the $\Lambda_b^{*0}(5920)$ state is 11.7σ , and the significance including systematic uncertainties is 10.2σ .

The fit biases and the validity of the statistical uncertainties are checked with pseudoexperiments where the PDF contains both signal and background components. The fit does not introduce any noticeable bias on the measurement of the masses. The mass uncertainty for $\Lambda_b^{*0}(5920)$ state is estimated correctly within 1% precision; however, the mass uncertainty for the $\Lambda_b^{*0}(5912)$ is underestimated by 4%. This factor is taken into account in the final result.

In summary, we report the observation of two narrow states in the $\Lambda_b^0 \pi^+ \pi^-$ mass spectrum, $\Lambda_b^{*0}(5912)$ and $\Lambda_b^{*0}(5920)$, with masses

$$M_{\Lambda_b^{*0}(5912)} = 5911.97 \pm 0.12 \pm 0.02 \pm 0.66 \text{ MeV}/c^2,$$

$$M_{\Lambda_b^{*0}(5920)} = 5919.77 \pm 0.08 \pm 0.02 \pm 0.66 \text{ MeV}/c^2,$$

where the first uncertainty is statistical, the second is systematic, and the third is the uncertainty due to knowledge of the Λ_b^0 mass. The values of the mass differences with respect to the Λ_b^0 mass, where most of the last uncertainty cancels and the remaining part is included in the systematic uncertainty, are

$$\Delta M_{\Lambda_b^{*0}(5912)} = 292.60 \pm 0.12(\text{stat}) \pm 0.04(\text{syst}) \text{ MeV}/c^2,$$

$$\Delta M_{\Lambda_b^{*0}(5920)} = 300.40 \pm 0.08(\text{stat}) \pm 0.04(\text{syst}) \text{ MeV}/c^2.$$

The signal yield for the $\Lambda_b^{*0}(5912)$ state is 17.6 ± 4.8 events, and the significance of the signal (including systematic uncertainty and trial factor in the mass range 5900–5950 MeV/ c^2) is 5.2 standard deviations. For the $\Lambda_b^{*0}(5920)$ state, the yield is 52.5 ± 8.1 events, and the significance is 10.2 standard deviations. The limits on the natural widths of these states are $\Gamma_{\Lambda_b^{*0}(5912)} < 0.66$ MeV (< 0.83 MeV) and $\Gamma_{\Lambda_b^{*0}(5920)} < 0.63$ MeV (< 0.75) at the 90% (95%) C.L.

The masses of Λ_b^{*0} states obtained in our analysis are 30–40 MeV/ c^2 higher than in the prediction using the constituent quark model [12] and 20–30 MeV/ c^2 lower than the predictions based on the relativistic quark model [11], modeling the color hyperfine interaction [14] and an approach based on the heavy quark effective theory [15]. Calculation involving a combined heavy quark and large number of colors expansion [9,10] gives a value roughly in agreement, although only the spin-averaged prediction is available. The earlier prediction based on the relativized quark potential model [13] matches well the absolute mass values for both states, but the Λ_b^0 mass prediction using this model is 35 MeV/ c^2 lower than the measured value.

We express our gratitude to our colleagues in the CERN accelerator departments for the excellent performance of the LHC. We thank the technical and administrative staff at

CERN and at the LHCb institutes and acknowledge support from the National Agencies: CAPES, CNPq, FAPERJ, and FINEP (Brazil); CERN; NSFC (China); CNRS/IN2P3 (France); BMBF, DFG, HGF, and MPG (Germany); SFI (Ireland); INFN (Italy); FOM and NWO (Netherlands); SCSR (Poland); ANCS (Romania); MinES of Russia and Rosatom (Russia); MICINN, XuntaGal, and GENCAT (Spain); SNSF and SER (Switzerland); NAS Ukraine (Ukraine); STFC (United Kingdom); NSF (USA). We also acknowledge the support received from the ERC under FP7 and the Region Auvergne.

-
- [1] V. Abazov *et al.* (D0 Collaboration), *Phys. Rev. Lett.* **99**, 052001 (2007).
- [2] T. Aaltonen *et al.* (CDF Collaboration), *Phys. Rev. Lett.* **99**, 052002 (2007).
- [3] V. Abazov *et al.* (D0 Collaboration), *Phys. Rev. Lett.* **101**, 232002 (2008).
- [4] T. Aaltonen *et al.* (CDF Collaboration), *Phys. Rev. D* **80**, 072003 (2009).
- [5] T. Aaltonen *et al.* (CDF Collaboration), *Phys. Rev. Lett.* **107**, 102001 (2011).
- [6] S. Chatrchyan *et al.* (CMS Collaboration), *Phys. Rev. Lett.* **108**, 252002 (2012).
- [7] T. Aaltonen *et al.* (CDF Collaboration), *Phys. Rev. Lett.* **99**, 202001 (2007).
- [8] T. Aaltonen *et al.* (CDF Collaboration), *Phys. Rev. D* **85**, 092011 (2012).
- [9] Z. Aziza Baccouche, C.-K. Chow, T. D. Cohen, and B. A. Gelman, *Nucl. Phys. A* **696**, 638 (2001).
- [10] Z. Aziza Baccouche, C.-K. Chow, T. D. Cohen, and B. A. Gelman, *Phys. Lett. B* **514**, 346 (2001).
- [11] D. Ebert, R. Faustov, and V. Galkin, *Phys. Lett. B* **659**, 612 (2008).
- [12] H. Garcilazo, J. Vijande, and A. Valcarce, *J. Phys. G* **34**, 961 (2007).
- [13] S. Capstick and N. Isgur, *Phys. Rev. D* **34**, 2809 (1986).
- [14] M. Karliner, B. Keren-Zur, H. J. Lipkin, and J. L. Rosner, *Ann. Phys. (N.Y.)* **324**, 2 (2009).
- [15] W. Roberts and M. Pervin, *Int. J. Mod. Phys. A* **23**, 2817 (2008).
- [16] A. A. Alves, Jr., *et al.* (LHCb Collaboration), *JINST* **3**, S08005 (2008).
- [17] V. Gligorov, C. Thomas, and M. Williams, Report No. LHCb-PUB-2011-016.
- [18] K. Nakamura *et al.* (Particle Data Group), *J. Phys. G* **37**, 075021 (2010).
- [19] R. Aaij *et al.* (LHCb Collaboration), *Phys. Lett. B* **708**, 241 (2012).
- [20] T. Sjöstrand, S. Mrenna, and P. Skands, *J. High Energy Phys.* **05** (2006) 026.
- [21] I. Belyaev *et al.*, in *Proceedings of the Nuclear Science Symposium 2010* (IEEE, New York, 2010), pp. 1155–1161.
- [22] D. J. Lange, *Nucl. Instrum. Methods Phys. Res., Sect. A* **462**, 152 (2001).
- [23] P. Golonka and Z. Was, *Eur. Phys. J. C* **45**, 97 (2006).
- [24] J. Allison *et al.* (GEANT4 Collaboration), *IEEE Trans. Nucl. Sci.* **53**, 270 (2006); S. Agostinelli *et al.* (GEANT4 Collaboration), *Nucl. Instrum. Methods Phys. Res., Sect. A* **506**, 250 (2003).
- [25] M. Clemencic, G. Corti, S. Easo, C. R. Jones, S. Miglioranza, M. Pappagallo, and P. Robbe, *J. Phys. Conf. Ser.* **331**, 032023 (2011).
- [26] R. Aaij *et al.* (LHCb Collaboration), *Phys. Lett. B* **708**, 241 (2012).
- [27] M. Pivk and F. L. Diberder, *Nucl. Instrum. Methods Phys. Res., Sect. A* **555**, 356 (2005).
- [28] E. Gross and O. Vitells, *Eur. Phys. J. C* **70**, 525 (2010).
-
- R. Aaij,³⁸ C. Abellan Beteta,^{33,n} A. Adametz,¹¹ B. Adeva,³⁴ M. Adinolfi,⁴³ C. Adrover,⁶ A. Affolder,⁴⁹ Z. Ajaltouni,⁵ J. Albrecht,³⁵ F. Alessio,³⁵ M. Alexander,⁴⁸ S. Ali,³⁸ G. Alkhazov,²⁷ P. Alvarez Cartelle,³⁴ A. A. Alves, Jr.,²² S. Amato,² Y. Amhis,³⁶ J. Anderson,³⁷ R. B. Appleby,⁵¹ O. Aquines Gutierrez,¹⁰ F. Archilli,^{18,35} A. Artamonov,³² M. Artuso,^{53,35} E. Aslanides,⁶ G. Auriemma,^{22,m} S. Bachmann,¹¹ J. J. Back,⁴⁵ V. Balagura,^{28,35} W. Baldini,¹⁶ R. J. Barlow,⁵¹ C. Barschel,³⁵ S. Barsuk,⁷ W. Barter,⁴⁴ A. Bates,⁴⁸ C. Bauer,¹⁰ Th. Bauer,³⁸ A. Bay,³⁶ J. Beddow,⁴⁸ I. Bediaga,¹ S. Belogurov,²⁸ K. Belous,³² I. Belyaev,²⁸ E. Ben-Haim,⁸ M. Benayoun,⁸ G. Bencivenni,¹⁸ S. Benson,⁴⁷ J. Benton,⁴³ R. Bernet,³⁷ M.-O. Bettler,¹⁷ M. van Beuzekom,³⁸ A. Bien,¹¹ S. Bifani,¹² T. Bird,⁵¹ A. Bizzeti,^{17,h} P. M. Bjørnstad,⁵¹ T. Blake,³⁵ F. Blanc,³⁶ C. Blanks,⁵⁰ J. Blouw,¹¹ S. Blusk,⁵³ A. Bobrov,³¹ V. Bocci,²² A. Bondar,³¹ N. Bondar,²⁷ W. Bonivento,¹⁵ S. Borghi,^{48,51} A. Borgia,⁵³ T. J. V. Bowcock,⁴⁹ C. Bozzi,¹⁶ T. Brambach,⁹ J. van den Brand,³⁹ J. Bressieux,³⁶ D. Brett,⁵¹ M. Britsch,¹⁰ T. Britton,⁵³ N. H. Brook,⁴³ H. Brown,⁴⁹ A. Büchler-Germann,³⁷ I. Burducea,²⁶ A. Bursche,³⁷ J. Buytaert,³⁵ S. Cadeddu,¹⁵ O. Callot,⁷ M. Calvi,^{20,j} M. Calvo Gomez,^{33,n} A. Camboni,³³ P. Campana,^{18,35} A. Carbone,¹⁴ G. Carboni,^{21,k} R. Cardinale,^{19,35,i} A. Cardini,¹⁵ L. Carson,⁵⁰ K. Carvalho Akiba,² G. Casse,⁴⁹ M. Cattaneo,³⁵ Ch. Cauet,⁹ M. Charles,⁵² Ph. Charpentier,³⁵ P. Chen,^{3,36} N. Chiapolini,³⁷ M. Chrzasczcz,²³ K. Ciba,³⁵ X. Cid Vidal,³⁴ G. Ciezarek,⁵⁰ P. E. L. Clarke,⁴⁷ M. Clemencic,³⁵ H. V. Cliff,⁴⁴ J. Closier,³⁵ C. Coca,²⁶ V. Coco,³⁸ J. Cogan,⁶ E. Cogneras,⁵ P. Collins,³⁵ A. Comerma-Montells,³³ A. Contu,⁵² A. Cook,⁴³ M. Coombes,⁴³ G. Corti,³⁵ B. Couturier,³⁵ G. A. Cowan,³⁶ D. Craik,⁴⁵ R. Currie,⁴⁷ C. D'Ambrosio,³⁵ P. David,⁸ P. N. Y. David,³⁸ I. De Bonis,⁴ K. De Bruyn,³⁸ S. De Capua,^{21,k} M. De Cian,³⁷ J. M. De Miranda,¹ L. De Paula,² P. De Simone,¹⁸ D. Decamp,⁴ M. Deckenhoff,⁹ H. Degaudenzi,^{36,35}

- L. Del Buono,⁸ C. Deplano,¹⁵ D. Derkach,^{14,35} O. Deschamps,⁵ F. Dettori,³⁹ J. Dickens,⁴⁴ H. Dijkstra,³⁵ P. Diniz Batista,¹ F. Domingo Bonal,^{33,n} S. Donleavy,⁴⁹ F. Dordei,¹¹ A. Dosil Suárez,³⁴ D. Dossett,⁴⁵ A. Dovbnya,⁴⁰ F. Dupertuis,³⁶ R. Dzhelyadin,³² A. Dziurda,²³ A. Dzyuba,²⁷ S. Easo,⁴⁶ U. Egede,⁵⁰ V. Egorychev,²⁸ S. Eidelman,³¹ D. van Eijk,³⁸ F. Eisele,¹¹ S. Eisenhardt,⁴⁷ R. Ekelhof,⁹ L. Eklund,⁴⁸ I. El Rifai,⁵ Ch. Elsasser,³⁷ D. Elsby,⁴² D. Esperante Pereira,³⁴ A. Falabella,^{16,14,e} C. Färber,¹¹ G. Fardell,⁴⁷ C. Farinelli,³⁸ S. Farry,¹² V. Fave,³⁶ V. Fernandez Albor,³⁴ M. Ferro-Luzzi,³⁵ S. Filippov,³⁰ C. Fitzpatrick,⁴⁷ M. Fontana,¹⁰ F. Fontanelli,^{19,i} R. Forty,³⁵ O. Francisco,² M. Frank,³⁵ C. Frei,³⁵ M. Frosini,^{17,f} S. Furcas,²⁰ A. Gallas Torreira,³⁴ D. Galli,^{14,c} M. Gandelman,² P. Gandini,⁵² Y. Gao,³ J.-C. Garnier,³⁵ J. Garofoli,⁵³ J. Garra Tico,⁴⁴ L. Garrido,³³ D. Gascon,³³ C. Gaspar,³⁵ R. Gauld,⁵² N. Gauvin,³⁶ M. Gersabeck,³⁵ T. Gershon,^{45,35} Ph. Ghez,⁴ V. Gibson,⁴⁴ V. V. Gligorov,³⁵ C. Göbel,⁵⁴ D. Golubkov,²⁸ A. Golutvin,^{50,28,35} A. Gomes,² H. Gordon,⁵² M. Grabalosa Gándara,³³ R. Graciani Diaz,³³ L. A. Granado Cardoso,³⁵ E. Graugés,³³ G. Graziani,¹⁷ A. Grecu,²⁶ E. Greening,⁵² S. Gregson,⁴⁴ O. Grünberg,⁵⁵ B. Gui,⁵³ E. Gushchin,³⁰ Yu. Guz,³² T. Gys,³⁵ C. Hadjivasilou,⁵³ G. Haefeli,³⁶ C. Haen,³⁵ S. C. Haines,⁴⁴ T. Hampson,⁴³ S. Hansmann-Menzemer,¹¹ N. Harnew,⁵² S. T. Harnew,⁴³ J. Harrison,⁵¹ P. F. Harrison,⁴⁵ T. Hartmann,⁵⁵ J. He,⁷ V. Heijne,³⁸ K. Hennessy,⁴⁹ P. Henrard,⁵ J. A. Hernando Morata,³⁴ E. van Herwijnen,³⁵ E. Hicks,⁴⁹ M. Hoballah,⁵ P. Hopchev,⁴ W. Hulsbergen,³⁸ P. Hunt,⁵² T. Huse,⁴⁹ R. S. Huston,¹² D. Hutchcroft,⁴⁹ D. Hynds,⁴⁸ V. Iakovenko,⁴¹ P. Ilten,¹² J. Imong,⁴³ R. Jacobsson,³⁵ A. Jaeger,¹¹ M. Jahjah Hussein,⁵ E. Jans,³⁸ F. Jansen,³⁸ P. Jaton,³⁶ B. Jean-Marie,⁷ F. Jing,³ M. John,⁵² D. Johnson,⁵² C. R. Jones,⁴⁴ B. Jost,³⁵ M. Kaballo,⁹ S. Kandybei,⁴⁰ M. Karacson,³⁵ T. M. Karbach,⁹ J. Keaveney,¹² I. R. Kenyon,⁴² U. Kerzel,³⁵ T. Ketel,³⁹ A. Keune,³⁶ B. Khanji,⁶ Y. M. Kim,⁴⁷ M. Knecht,³⁶ O. Kochebina,⁷ I. Komarov,²⁹ R. F. Koopman,³⁹ P. Koppenburg,³⁸ M. Korolev,²⁹ A. Kozlinskiy,³⁸ L. Kravchuk,³⁰ K. Kreplin,¹¹ M. Kreps,⁴⁵ G. Krocker,¹¹ P. Krokovny,³¹ F. Kruse,⁹ K. Kruzelecki,³⁵ M. Kucharczyk,^{20,23,35,j} V. Kudryavtsev,³¹ T. Kvaratskheliya,^{28,35} V. N. La Thi,³⁶ D. Lacarrere,³⁵ G. Lafferty,⁵¹ A. Lai,¹⁵ D. Lambert,⁴⁷ R. W. Lambert,³⁹ E. Lanciotti,³⁵ G. Lanfranchi,¹⁸ C. Langenbruch,³⁵ T. Latham,⁴⁵ C. Lazzeroni,⁴² R. Le Gac,⁶ J. van Leerdam,³⁸ J.-P. Lees,⁴ R. Lefèvre,⁵ A. Leflat,^{29,35} J. Lefrançois,⁷ O. Leroy,⁶ T. Lesiak,²³ L. Li,³ Y. Li,³ L. Li Gioi,⁵ M. Lieng,⁹ M. Liles,⁴⁹ R. Lindner,³⁵ C. Linn,¹¹ B. Liu,³ G. Liu,³⁵ J. von Loeben,²⁰ J. H. Lopes,² E. Lopez Asamar,³³ N. Lopez-March,³⁶ H. Lu,³ J. Luisier,³⁶ A. Mac Raighne,⁴⁸ F. Machefert,⁷ I. V. Machikhiliyan,^{4,28} F. Maciuc,¹⁰ O. Maev,^{27,35} J. Magnin,¹ S. Malde,⁵² R. M. D. Mamunur,³⁵ G. Manca,^{15,d} G. Mancinelli,⁶ N. Mangiafave,⁴⁴ U. Marconi,¹⁴ R. Märki,³⁶ J. Marks,¹¹ G. Martellotti,²² A. Martens,⁸ L. Martin,⁵² A. Martín Sánchez,⁷ M. Martinelli,³⁸ D. Martinez Santos,³⁵ A. Massafferri,¹ Z. Mathe,¹² C. Matteuzzi,²⁰ M. Matveev,²⁷ E. Maurice,⁶ B. Maynard,⁵³ A. Mazurov,^{16,30,35} J. McCarthy,⁴² G. McGregor,⁵¹ R. McNulty,¹² M. Meissner,¹¹ M. Merk,³⁸ J. Merkel,⁹ D. A. Milanes,¹³ M.-N. Minard,⁴ J. Molina Rodriguez,⁵⁴ S. Monteil,⁵ D. Moran,¹² P. Morawski,²³ R. Mountain,⁵³ I. Mous,³⁸ F. Muheim,⁴⁷ K. Müller,³⁷ R. Muresan,²⁶ B. Muryn,²⁴ B. Muster,³⁶ J. Mylroie-Smith,⁴⁹ P. Naik,⁴³ T. Nakada,³⁶ R. Nandakumar,⁴⁶ I. Nasteva,¹ M. Needham,⁴⁷ N. Neufeld,³⁵ A. D. Nguyen,³⁶ C. Nguyen-Mau,^{36,o} M. Nicol,⁷ V. Niess,⁵ N. Nikitin,²⁹ T. Nikodem,¹¹ A. Nomerotski,^{52,35} A. Novoselov,³² A. Oblakowska-Mucha,²⁴ V. Obraztsov,³² S. Oggero,³⁸ S. Ogilvy,⁴⁸ O. Okhrimenko,⁴¹ R. Oldeman,^{15,35,d} M. Orlandea,²⁶ J. M. Otalora Goicochea,² P. Owen,⁵⁰ B. K. Pal,⁵³ J. Palacios,³⁷ A. Palano,^{13,b} M. Palutan,¹⁸ J. Panman,³⁵ A. Papanestis,⁴⁶ M. Pappagallo,⁴⁸ C. Parkes,⁵¹ C. J. Parkinson,⁵⁰ G. Passaleva,¹⁷ G. D. Patel,⁴⁹ M. Patel,⁵⁰ G. N. Patrick,⁴⁶ C. Patrignani,^{19,i} C. Pavel-Nicorescu,²⁶ A. Pazos Alvarez,³⁴ A. Pellegrino,³⁸ G. Penso,^{22,l} M. Pepe Altarelli,³⁵ S. Perazzini,^{14,c} D. L. Perego,^{20,j} E. Perez Trigo,³⁴ A. Pérez-Calero Yzquierdo,³³ P. Perret,⁵ M. Perrin-Terrin,⁶ G. Pessina,²⁰ A. Petrolini,^{19,i} A. Phan,⁵³ E. Picatoste Olloqui,³³ B. Pie Valls,³³ B. Pietrzyk,⁴ T. Pilař,⁴⁵ D. Pinci,²² R. Plackett,⁴⁸ S. Playfer,⁴⁷ M. Plo Casasus,³⁴ F. Polci,⁸ G. Polok,²³ A. Poluektov,^{45,31} E. Polcarpo,² D. Popov,¹⁰ B. Popovici,²⁶ C. Potterat,³³ A. Powell,⁵² J. Prisciandaro,³⁶ V. Pugatch,⁴¹ A. Puig Navarro,³³ W. Qian,⁵³ J. H. Rademacker,⁴³ B. Rakotomiamanana,³⁶ M. S. Rangel,² I. Raniuk,⁴⁰ G. Raven,³⁹ S. Redford,⁵² M. M. Reid,⁴⁵ A. C. dos Reis,¹ S. Ricciardi,⁴⁶ A. Richards,⁵⁰ K. Rinnert,⁴⁹ D. A. Roa Romero,⁵ P. Robbe,⁷ E. Rodrigues,^{48,51} F. Rodrigues,² P. Rodriguez Perez,³⁴ G. J. Rogers,⁴⁴ S. Roiser,³⁵ V. Romanovsky,³² M. Rosello,^{33,n} J. Rouvinet,³⁶ T. Ruf,³⁵ H. Ruiz,³³ G. Sabatino,^{21,k} J. J. Saborido Silva,³⁴ N. Sagidova,²⁷ P. Sail,⁴⁸ B. Saitta,^{15,d} C. Salzmann,³⁷ B. Sanmartin Sedes,³⁴ M. Sannino,^{19,i} R. Santacesaria,²² C. Santamarina Rios,³⁴ R. Santinelli,³⁵ E. Santovetti,^{21,k} M. Sapunov,⁶ A. Sarti,^{18,l} C. Satriano,^{22,m} A. Satta,²¹ M. Savrie,^{16,e} D. Savrina,²⁸ P. Schaack,⁵⁰ M. Schiller,³⁹ H. Schindler,³⁵ S. Schleich,⁹ M. Schlupp,⁹ M. Schmelling,¹⁰ B. Schmidt,³⁵ O. Schneider,³⁶ A. Schopper,³⁵ M.-H. Schune,⁷ R. Schwemmer,³⁵ B. Sciascia,¹⁸ A. Sciubba,^{18,l} M. Seco,³⁴ A. Semennikov,²⁸ K. Senderowska,²⁴ I. Sepp,⁵⁰ N. Serra,³⁷ J. Serrano,⁶ P. Seyfert,¹¹ M. Shapkin,³² I. Shapoval,^{40,35} P. Shatalov,²⁸ Y. Shcheglov,²⁷

T. Shears,⁴⁹ L. Shekhtman,³¹ O. Shevchenko,⁴⁰ V. Shevchenko,²⁸ A. Shires,⁵⁰ R. Silva Coutinho,⁴⁵ T. Skwarnicki,⁵³ N. A. Smith,⁴⁹ E. Smith,^{52,46} M. Smith,⁵¹ K. Sobczak,⁵ F. J. P. Soler,⁴⁸ A. Solomin,⁴³ F. Soomro,^{18,35} D. Souza,⁴³ B. Souza De Paula,² B. Spaan,⁹ A. Sparkes,⁴⁷ P. Spradlin,⁴⁸ F. Stagni,³⁵ S. Stahl,¹¹ O. Steinkamp,³⁷ S. Stoica,²⁶ S. Stone,^{53,35} B. Storaci,³⁸ M. Straticiuc,²⁶ U. Straumann,³⁷ V. K. Subbiah,³⁵ S. Swientek,⁹ M. Szczekowski,²⁵ P. Szczypka,³⁶ T. Szumlak,²⁴ S. T'Jampens,⁴ M. Teklishyn,⁷ E. Teodorescu,²⁶ F. Teubert,³⁵ C. Thomas,⁵² E. Thomas,³⁵ J. van Tilburg,¹¹ V. Tisserand,⁴ M. Tobin,³⁷ S. Tolks,³⁹ S. Topp-Joergensen,⁵² N. Torr,⁵² E. Tournefier,^{4,50} S. Tourneur,³⁶ M. T. Tran,³⁶ A. Tsaregorodtsev,⁶ N. Tuning,³⁸ M. Ubeda Garcia,³⁵ A. Ukleja,²⁵ U. Uwer,¹¹ V. Vagnoni,¹⁴ G. Valenti,¹⁴ R. Vazquez Gomez,³³ P. Vazquez Regueiro,³⁴ S. Vecchi,¹⁶ J. J. Velthuis,⁴³ M. Veltri,^{17,g} M. Vesterinen,³⁵ B. Viaud,⁷ I. Videau,⁷ D. Vieira,² X. Vilasis-Cardona,^{33,n} J. Visniakov,³⁴ A. Vollhardt,³⁷ D. Volyanskyy,¹⁰ D. Voong,⁴³ A. Vorobyev,²⁷ V. Vorobyev,³¹ C. Voß,⁵⁵ H. Voss,¹⁰ R. Waldi,⁵⁵ R. Wallace,¹² S. Wandernoth,¹¹ J. Wang,⁵³ D. R. Ward,⁴⁴ N. K. Watson,⁴² A. D. Webber,⁵¹ D. Websdale,⁵⁰ M. Whitehead,⁴⁵ J. Wicht,³⁵ D. Wiedner,¹¹ L. Wiggers,³⁸ G. Wilkinson,⁵² M. P. Williams,^{45,46} M. Williams,⁵⁰ F. F. Wilson,⁴⁶ J. Wishahi,⁹ M. Witek,²³ W. Witzeling,³⁵ S. A. Wotton,⁴⁴ S. Wright,⁴⁴ S. Wu,³ K. Wyllie,³⁵ Y. Xie,⁴⁷ F. Xing,⁵² Z. Xing,⁵³ Z. Yang,³ R. Young,⁴⁷ X. Yuan,³ O. Yushchenko,³² M. Zangoli,¹⁴ M. Zavertyaev,^{10,a} F. Zhang,³ L. Zhang,⁵³ W. C. Zhang,¹² Y. Zhang,³ A. Zhelezov,¹¹ L. Zhong,³ and A. Zvyagin³⁵

(LHCb Collaboration)

¹Centro Brasileiro de Pesquisas Físicas (CBPF), Rio de Janeiro, Brazil

²Universidade Federal do Rio de Janeiro (UFRJ), Rio de Janeiro, Brazil

³Center for High Energy Physics, Tsinghua University, Beijing, China

⁴LAPP, Université de Savoie, CNRS/IN2P3, Annecy-Le-Vieux, France

⁵Clermont Université, Université Blaise Pascal, CNRS/IN2P3, LPC, Clermont-Ferrand, France

⁶CPM, Aix-Marseille Université, CNRS/IN2P3, Marseille, France

⁷LAL, Université Paris-Sud, CNRS/IN2P3, Orsay, France

⁸LPNHE, Université Pierre et Marie Curie, Université Paris Diderot, CNRS/IN2P3, Paris, France

⁹Fakultät Physik, Technische Universität Dortmund, Dortmund, Germany

¹⁰Max-Planck-Institut für Kernphysik (MPIK), Heidelberg, Germany

¹¹Physikalisches Institut, Ruprecht-Karls-Universität Heidelberg, Heidelberg, Germany

¹²School of Physics, University College Dublin, Dublin, Ireland

¹³Sezione INFN di Bari, Bari, Italy

¹⁴Sezione INFN di Bologna, Bologna, Italy

¹⁵Sezione INFN di Cagliari, Cagliari, Italy

¹⁶Sezione INFN di Ferrara, Ferrara, Italy

¹⁷Sezione INFN di Firenze, Firenze, Italy

¹⁸Laboratori Nazionali dell'INFN di Frascati, Frascati, Italy

¹⁹Sezione INFN di Genova, Genova, Italy

²⁰Sezione INFN di Milano Bicocca, Milano, Italy

²¹Sezione INFN di Roma Tor Vergata, Roma, Italy

²²Sezione INFN di Roma La Sapienza, Roma, Italy

²³Henryk Niewodniczanski Institute of Nuclear Physics Polish Academy of Sciences, Kraków, Poland

²⁴AGH University of Science and Technology, Kraków, Poland

²⁵Soltan Institute for Nuclear Studies, Warsaw, Poland

²⁶Horia Hulubei National Institute of Physics and Nuclear Engineering, Bucharest-Magurele, Romania

²⁷Petersburg Nuclear Physics Institute (PNPI), Gatchina, Russia

²⁸Institute of Theoretical and Experimental Physics (ITEP), Moscow, Russia

²⁹Institute of Nuclear Physics, Moscow State University (SINP MSU), Moscow, Russia

³⁰Institute for Nuclear Research of the Russian Academy of Sciences (INR RAN), Moscow, Russia

³¹Budker Institute of Nuclear Physics (SB RAS) and Novosibirsk State University, Novosibirsk, Russia

³²Institute for High Energy Physics (IHEP), Protvino, Russia

³³Universitat de Barcelona, Barcelona, Spain

³⁴Universidad de Santiago de Compostela, Santiago de Compostela, Spain

³⁵European Organization for Nuclear Research (CERN), Geneva, Switzerland

³⁶Ecole Polytechnique Fédérale de Lausanne (EPFL), Lausanne, Switzerland

³⁷Physik-Institut, Universität Zürich, Zürich, Switzerland

³⁸Nikhef National Institute for Subatomic Physics, Amsterdam, Netherlands

³⁹Nikhef National Institute for Subatomic Physics and VU University Amsterdam, Amsterdam, Netherlands

- ⁴⁰*NSC Kharkiv Institute of Physics and Technology (NSC KIPT), Kharkiv, Ukraine*
⁴¹*Institute for Nuclear Research of the National Academy of Sciences (KINR), Kyiv, Ukraine*
⁴²*University of Birmingham, Birmingham, United Kingdom*
⁴³*H. H. Wills Physics Laboratory, University of Bristol, Bristol, United Kingdom*
⁴⁴*Cavendish Laboratory, University of Cambridge, Cambridge, United Kingdom*
⁴⁵*Department of Physics, University of Warwick, Coventry, United Kingdom*
⁴⁶*STFC Rutherford Appleton Laboratory, Didcot, United Kingdom*
⁴⁷*School of Physics and Astronomy, University of Edinburgh, Edinburgh, United Kingdom*
⁴⁸*School of Physics and Astronomy, University of Glasgow, Glasgow, United Kingdom*
⁴⁹*Oliver Lodge Laboratory, University of Liverpool, Liverpool, United Kingdom*
⁵⁰*Imperial College London, London, United Kingdom*
⁵¹*School of Physics and Astronomy, University of Manchester, Manchester, United Kingdom*
⁵²*Department of Physics, University of Oxford, Oxford, United Kingdom*
⁵³*Syracuse University, Syracuse, New York, USA*
⁵⁴*Pontifícia Universidade Católica do Rio de Janeiro (PUC-Rio), Rio de Janeiro, Brazil, associated to Universidade Federal do Rio de Janeiro (UFRJ), Rio de Janeiro, Brazil*
⁵⁵*Institut für Physik, Universität Rostock, Rostock, Germany, associated to Physikalisches Institut, Ruprecht-Karls-Universität Heidelberg, Heidelberg, Germany*

^aAlso at P.N. Lebedev Physical Institute, Russian Academy of Science (LPI RAS), Moscow, Russia.

^bAlso at Università di Bari, Bari, Italy.

^cAlso at Università di Bologna, Bologna, Italy.

^dAlso at Università di Cagliari, Cagliari, Italy.

^eAlso at Università di Ferrara, Ferrara, Italy.

^fAlso at Università di Firenze, Firenze, Italy.

^gAlso at Università di Urbino, Urbino, Italy.

^hAlso at Università di Modena e Reggio Emilia, Modena, Italy.

ⁱAlso at Università di Genova, Genova, Italy.

^jAlso at Università di Milano Bicocca, Milano, Italy.

^kAlso at Università di Roma Tor Vergata, Roma, Italy.

^lAlso at Università di Roma La Sapienza, Roma, Italy.

^mAlso at Università della Basilicata, Potenza, Italy.

ⁿAlso at LIFAELS, La Salle, Universitat Ramon Llull, Barcelona, Spain.

^oAlso at Hanoi University of Science, Hanoi, Vietnam.